European Radiology (2019) 29:4544–4554
https://doi.org/10.1007/s00330-019-06042-w

CHEST

Agreement between magnetic resonance imaging and computed tomography in the postnatal evaluation of congenital lung malformations: a pilot study

Salvatore Zirpoli[1] · Alice Marianna Munari[1] · Alessandra Primolevo[2] · Marco Scarabello[3] · Sara Costanzo[4] · Andrea Farolfi[5] · Gianluca Lista[6] · Elena Zoia[7] · Gian Vincenzo Zuccotti[5] · Giovanna Riccipetitoni[4] · Andrea Righini[1]

Received: 27 August 2018 / Revised: 20 December 2018 / Accepted: 24 January 2019 / Published online: 22 February 2019

Abstract

Objectives To compare postnatal magnetic resonance imaging (MRI) with the reference standard computed tomography (CT) in the identification of the key features for diagnosing different types of congenital lung malformation (CLM).

Methods Respiratory-triggered T2-weighted single-shot turbo spin echo (ss-TSE), respiratory-triggered T1-weighted turbo field echo (TFE), balanced fast field echo (BFFE), and T2-weighted MultiVane sequences were performed at 1.5 T on 20 patients prospectively enrolled. Two independent radiologists examined the postnatal CT and MRI evaluating the presence of cysts, hyperinflation, solid component, abnormal arteries and/or venous drainage, and bronchocele. Diagnostic performance of MRI was calculated and the agreement between the findings was assessed using the McNemar-Bowker test. Interobserver agreement was measured with the kappa coefficient.

Results CT reported five congenital pulmonary airway malformations (CPAMs), eight segmental bronchial atresias, five bronchopulmonary sequestrations (BPS), one congenital lobar overinflation, one bronchogenic cyst, and three hybrid lesions. MRI reported the correct diagnosis in 19/20 (95%) patients and the malformation was correctly classified in 22/23 cases (96%). MRI correctly identified all the key findings described on the CT except for the abnormal vascularization (85.7% sensitivity, 100% specificity, 100% PPV, 94.1% NPV, 95% accuracy for arterial vessels; 57.1% sensitivity, 100% specificity, 100% PPV, 84.2% NPV, 87% accuracy for venous drainage).

Conclusions MRI can represent an effective alternative to CT in the postnatal assessment of CLM. In order to further narrow the gap with CT, the use of contrast material and improvements in sequence design are needed to obtain detailed information on vascularization, which is essential for surgical planning.

Key Points

- *Congenital lung malformations (CLMs) can be effectively studied by MRI avoiding radiation exposure.*
- *Crucial features of CLM have similar appearance when comparing CT with MRI.*
- *MRI performs very well in CLM except for aberrant vessel detection and characterization.*

Keywords Lung malformation · Cystic adenomatoid, congenital · Magnetic resonance · Pediatrics · Bronchopulmonary sequestration

✉ Salvatore Zirpoli
salvatore.zirpoli@asst-fbf-sacco.it

[1] Pediatric Radiology and Neuroradiology, ASST Fatebenefratelli-Sacco Milano, Children's Hospital V. Buzzi, Via Castelvetro 32, 20154 Milan, Italy

[2] Radiology, Ospedale della Murgia F. Perinei, Altamura, BA, Italy

[3] Postgraduate School in Radiodiagnostics, Università degli Studi di Milano, Via Festa del Perdono 7, 20122 Milan, Italy

[4] Department of Pediatric Surgery, ASST Fatebenefratelli-Sacco Milano, Children's Hospital V. Buzzi, Via Castelvetro 32, 20154 Milan, Italy

[5] Department of Pediatrics, ASST Fatebenefratelli-Sacco Milano, Children's Hospital V. Buzzi, Via Castelvetro 32, 20154 Milan, Italy

[6] Neonatal Intensive Care Unit, ASST Fatebenefratelli-Sacco Milano, Children's Hospital V. Buzzi, Via Castelvetro 32, 20154 Milan, Italy

[7] Pediatric Intensive Care Unit, ASST Fatebenefratelli-Sacco Milano, Children's Hospital V. Buzzi, Via Castelvetro 32, 20154 Milan, Italy

Abbreviations

BPS	Bronchopulmonary sequestration
CLM	Congenital lung malformation
CLO	Congenital lobar overinflation
CPAM	Congenital pulmonary airway malformation
CT	Computed tomography
MRI	Magnetic resonance imaging

Introduction

Congenital lung malformations (CLMs) represent a large spectrum of abnormalities of the pulmonary development with different clinical and radiological features; they can be found as isolated malformations, separately affecting bronchi, lung parenchyma, pulmonary arterial supply, and venous drainage; otherwise, they can appear as hybrid malformations, merging features of different anomalies.

The most common CLMs are congenital pulmonary airway malformations (CPAMs), bronchopulmonary sequestration (BPS), bronchial atresia, bronchogenic cyst, and congenital lobar overinflation (CLO); all together they account for more than 95% of all lung malformations. The annual incidence of CLM is between 30 and 42 cases per ten thousand newborns [1–5]. The etiology is still unknown, although the most accepted theory hypothesizes that they derive from an aberrant obstruction of the developing bronchus. Variations in onset time, grade, and location of the obstruction can explain the variability in the severity of the resulting distal lung dysplasia [1, 2].

Nowadays in developed countries, almost all CLMs are diagnosed in the prenatal period [6], but they show great variability in their outcomes and clinical evolution. For these reasons, all patients with a prenatal diagnosis of CLM undergo postnatal contrast-enhanced chest computed tomography (CT) to confirm and better characterize the lung abnormalities. Postnatal CT is generally performed between 3 and 6 months of life, whereas only in symptomatic patients CT is performed in the first days or in the first month of life [7].

CT is considered the gold standard technique to study CLM, providing the most detailed information for therapeutic management [8–10], especially thanks to supplemental multiplanar and three-dimensional reconstructions [11]; nevertheless, it carries the risks deriving from ionizing radiation, particularly relevant in this age group [12–14].

For the last few years, radiation-free imaging techniques, such as chest ultrasound and magnetic resonance imaging (MRI), have been used more and more to evaluate pediatric pulmonary and mediastinal diseases and the indications for the use of MRI instead of CT in pediatric lung diseases have increased. Few studies have been published regarding the comparison between MRI and CT in the study of pneumonia and its complications, tumors, and cystic and non-cystic fibroses [15–19]. However, comparative studies between MRI and CT in postnatal evaluation of CLM have not been reported yet.

The purpose of this pilot prospective study is to compare postnatal CT and MRI in the postnatal evaluation of CLM.

Materials and methods

This single-center prospective study was approved by the Institutional Ethics Committee. Informed written consent was prospectively obtained from the parents of all children.

Study population

From November 2013 to August 2017, all consecutive patients with a prenatal diagnosis of CLM, confirmed by prenatal ultrasound and subsequent prenatal MRI examinations and listed for a postnatal CT scan, were enrolled.

All children underwent postnatal MRI and CT scans with sedation (deep sedation in spontaneously breathing patients, obtained with thiopental (Sodium Pentothal), at the dose of 3–7 mg/kg, according to our hospital protocol). Sedation time, for our purposes, was not different between CT and MRI since patients spontaneously transition from a deep sedation to a shallower sleep-like state (after the initial effective dose) that was equally effective in providing motion-free images. All patients gradually awakened from sedation under direct monitoring. The scanned area extended from the thoracic inlet to the plane of the renal arteries for both techniques. Time lapse between MRI and CT was 0–186 days (median 42.5 days); in nine patients, both MRI and CT were performed on the same day, under the same round of sedation.

MRI protocol

All children underwent a 1.5-T MRI (Achieva Dual; Philips) with a two-channel body coil (SENSE FLEX M) in supine position without contrast injection, using 3–4-mm slice thickness sequences.

MRI images were obtained with the following sequences: respiratory-triggered T2-weighted single-shot turbo spin echo (ss-TSE) sequences with short decreasing TE in axial, coronal, and sagittal planes (TR/TE, 1100 ms/120-70-60 ms; flip angle, 90°; in-plane resolution 0.9 mm^2); respiratory-triggered T1-weighted turbo field echo (TFE) inversion prepulse sequences (TR/TE, 10 ms/4.6 ms; flip angle, 15°; in-plane resolution 1.1 mm^2) in axial planes; and balanced fast field echo (BFFE) sequences (TR/TE, 3.9 ms/1.96 ms; flip angle, 60°; in-plane resolution 0.9 mm^2) in axial and coronal planes.

In four patients, T2-weighted MultiVane sequences (TR/TE, 1850 ms/100 ms; isotropic FOV and voxel; flip angle, 90°; in-plane resolution 1.1 mm^2) were also performed, along with fat suppression (TR/TE, 2285 ms/80 ms; isotropic FOV

and voxel; flip angle, 90°; in-plane resolution 1.1 mm^2) in axial and coronal planes.

The mean scan time was about 30 min.

CT protocol

All CT studies were performed with a 16-slice CT scanner (Siemens, Somatom Sensation 16 CT scanner) with a single acquisition after contrast injection. All CT studies were performed with the following parameters: 0.75-mm collimation, 80 kVp, 25–40 mA (related to the patient's weight) with CARE Dose 4D, tube rotation time of 0.5 s, and pitch of 1.0; computed tomography dose index (CTDIvol) range was 0.7–1.1 mGy and dose-length product (DLP) range was 8–15 mGy cm.

CT images were reconstructed with a 1–2-mm slice thickness in axial, coronal, and sagittal planes, with pulmonary and mediastinal window. Minimum intensity projection (MinIP) and volume rendering (VR) reconstructions were also performed.

All patients received a nonionic contrast medium (Iopromide (Ultravist) 370 mg I/mL, Bayer) at the dose of 2 mL/kg and injection rate of 1–2 mL/s, using a dual-head injector (Ulrich Medizintechnik). The contrast injection was followed by a saline chaser of 4–8 mL at the same injection rate. Scan was set to start after the end of contrast injection.

MRI and CT image analysis

Two independent pediatric radiologists, with 10 and 5 years of experience in pediatric thoracic radiology respectively, independently reviewed MRI and CT examinations of each patient in two different sessions filling a database. All MRI and CT images were analyzed on a PACS workstation (Impax, Agfa-Gevaert) after removing patients' identifying information. Both pediatric radiologists first reviewed all MRI images while the corresponding CT images were reviewed in a different session. Patients' examinations were displayed in random order during both reading sessions, which were separated by 4 weeks to avoid recall bias.

The observers were blinded to prenatal tests, the evolution of malformation in prenatal time, and postnatal clinical evaluation or diagnostic tests (ultrasound, chest X-ray).

The presence of CLM was assessed on a per-lobe and per-lung basis. When multiple lung malformations were present in the same patient, they were counted as separate when affecting different lobes or presenting different morphological features.

The agreement between MRI and CT was assessed by evaluating the site of malformation (side, lobe, or mediastinum) and the presence or absence of the following elements, considered relevant for diagnosis:

1. presence of cysts
2. presence of overinflation
3. presence of solid component
4. presence and origin of abnormal arteries and/or venous drainage
5. presence of bronchocele

Once all these elements were evaluated, both radiologists classified the type of CLM according to the following description.

Congenital pulmonary airway malformation is subdivided into type 1 that shows cysts greater than 2 cm with presumed bronchial/bronchiolar origin; type 2 that shows cysts less than 2 cm with presumed bronchiolar origin; and type 3 that appears solid or shows very small cysts (< 0.2 cm) with presumed bronchiolar/alveolar origin.

Segmental bronchial atresia is characterized by atresia or stenosis of a lobar, segmental, or subsegmental bronchus at or near its origin. This results in a blind-ended atretic proximal bronchus, the distal portion of which dilates with a variable amount of mucus, hence the term "mucocele." Bronchopulmonary sequestrations are defined as solid, unaerated lesions; extralobar BPS are usually located within the left hemithorax and appear as wedge-shaped masses delimited by pleura and often located below the normally formed lung.

Congenital lobar overinflation is characterized by a hyperinflated lobe with attenuated pulmonary vessels.

Bronchogenic cysts are well-defined hypoattenuating lesions with uniform fluid attenuation (0–20 Hounsfield units) on CT and always demonstrate high signal intensity on T2-weighted MRI images [5, 8].

The reference standard used was the CT reading performed by the more experienced pediatric radiologist with 10 years of experience in thoracic CT imaging.

Statistical analysis

To determine the agreement between MRI and CT findings, the *kappa statistic* was used. The diagnostic performance of MRI versus the reference standard CT in the evaluation of the relevant elements for diagnosis previously listed was expressed in terms of sensitivity, specificity, accuracy, positive predictive value (PPV), and negative predictive value (NPV). The analysis was performed considering each lung as an independent unit.

The interobserver agreement regarding the previously mentioned relevant elements for diagnosis of the CLM was measured using the *kappa statistic*. The McNemar-Bowker test was employed to check for marginal inhomogeneity for categorical variables with more than two traits.

Results

Patient characteristics

Twenty patients (10 males and 10 females) were enrolled; the age of the population ranged between 0 and 8 months (median age 95 days; range 12–322 days).

CT and MRI findings

CT findings, taken as reference standard, are described in Table 1.

On the CT, we found 23 malformations, as two patients had bilateral lung malformations and one had two different unassociated lung malformations on the same side but in different lobes.

We reported five CPAMs (four CPAM type 2 and one CPAM type 1) (Fig. 1), eight segmental bronchial atresia (Fig. 2), five BPS (Fig. 3), one CLO (Fig. 4), one bronchogenic cyst (Fig. 5), and three hybrid lesions (two BPS + CPAM type 2 (Fig. 6), one CPAM type 2 + bronchial atresia).

Eleven out of 23 (48%) malformations were located in the right hemithorax, one malformation was located in the mediastinum; 21/23 (91%) malformations involved a single pulmonary lobe, while two CLM presented a bilobar involvement; the lower lobe was the most commonly involved (17/23; 74%). MRI correctly identified all the findings described on the CT except for the abnormal vascularization: considering the seven cases of malformations associated with abnormal vasculature, MRI correctly identified the abnormal vessels in only four cases (57%), while in two cases (patient numbers 6 and 12) MRI was not able to identify the venous

Table 1 CT results. *UL*, upper lobe; *LL*, lower lobe; *Lin*, lingula; *ML*, middle lobe; *CPAM*, congenital pulmonary airway malformation; *CLO*, congenital lobar overinflation

Patients	Localization		Presence of						Malformation
	Side	Lobe	Cyst	Hyperinflation	Solid component	Abnormal arteries	Abnormal venous drainage	Bronchocele	
1	Right	UL, LL	Yes	No	No	No	No	No	CPAM
	Left	Lin, LL	Yes	No	No	No	No	No	CPAM
2	Right	LL	Yes	No	Yes	Thoracic aorta	Pulmonary circulation	No	Hybrid lesion (CPAM-sequestration)
	Left	LL	Yes	No	No	No	No	No	CPAM
3	Right	LL	No	Yes	No	No	No	Yes	Bronchial atresia
4	Left	LL	No	Yes	No	No	No	Yes	Bronchial atresia
5	Left	LL	Yes	No	Yes	Thoracic aorta	Pulmonary circulation	No	Hybrid lesion (CPAM - sequestration)
6	Right	LL	No	No	Yes	Thoracic aorta	Systemic circulation	No	Sequestration
7	Right	LL	No	No	Yes	Celiac trunk	Pulmonary circulation	No	Sequestration
8	Left	UL	No	Yes	No	No	No	No	CLO
9	Left	LL	No	Yes	No	No	No	Yes	Bronchial atresia
10	Left	LL	Yes	Yes	No	No	No	Yes	Hybrid lesion (CPAM-bronchial atresia)
11	Right	UL	Yes	No	No	No	No	No	CPAM
	Right	ML	No	Yes	No	No	No	Yes	Bronchial atresia
12	Left	LL	No	No	Yes	Thoracic aorta	Systemic circulation	No	Sequestration
13	Mediastinum		Yes	No	No	No	No	No	Bronchogenic cyst
14	Right	LL	Yes	No	No	No	No	No	CPAM
15	Left	LL	No	No	Yes	Thoracic aorta	Systemic circulation	No	Sequestration
16	Right	LL	No	Yes	No	No	No	Yes	Bronchial atresia
17	Left	UL	No	Yes	No	No	No	Yes	Bronchial atresia
18	Left	LL	No	No	Yes	Thoracic aorta	Systemic circulation	No	Sequestration
19	Right	LL	No	Yes	No	No	No	Yes	Bronchial atresia
20	Right	UL	No	Yes	No	No	No	Yes	Bronchial atresia

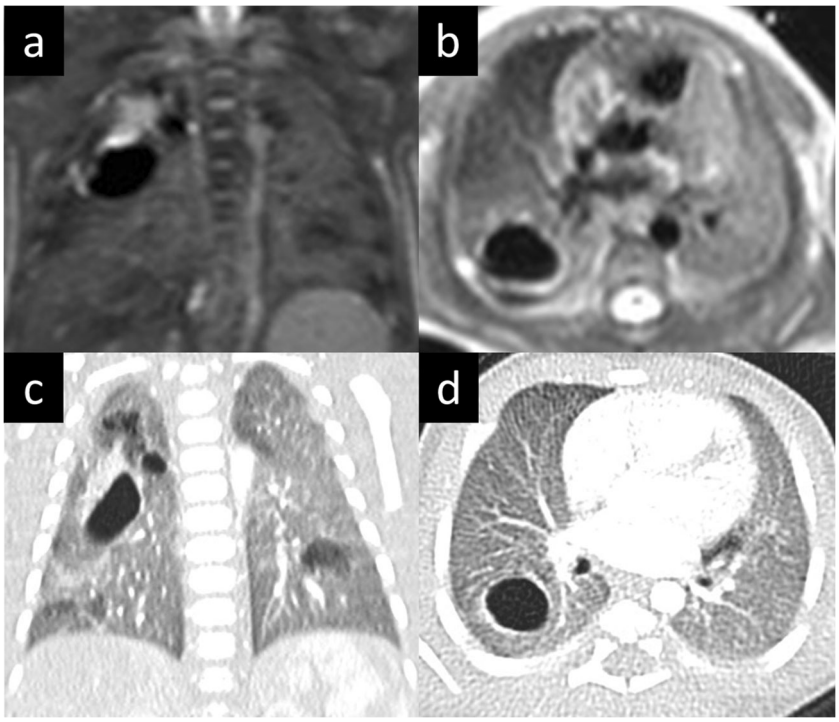

Fig. 1 CT and MR images of CPAM type 2. Coronal (**a**) and axial (**b**) MRss-TSE T2-w images compared with coronal (**c**) and axial (**d**) CT images

drainage and in one case (patient number 15) both the abnormal arterial and venous vessels were not identified.

In this last case, MRI was not able to assign a definitive diagnosis suggesting a possible sequestration or CPAM solid lesion (type 3 based on Stocker's classification [20]) or hybrid lesion. In the remaining 19 patients (95%) (22/23 malformations, 96%), MRI diagnoses were the same as those of CT.

Correlation of CT and MRI findings

The agreement on the localization of CLM between MRI and CT was excellent (Cohen's $k = 1.00$; $p < 0.001$).

In the evaluation of location and presence of cysts, overinflation, bronchocele, and solid components, there was a complete agreement between MRI and CT findings in every patient ($k = 1.00$, Table 2).

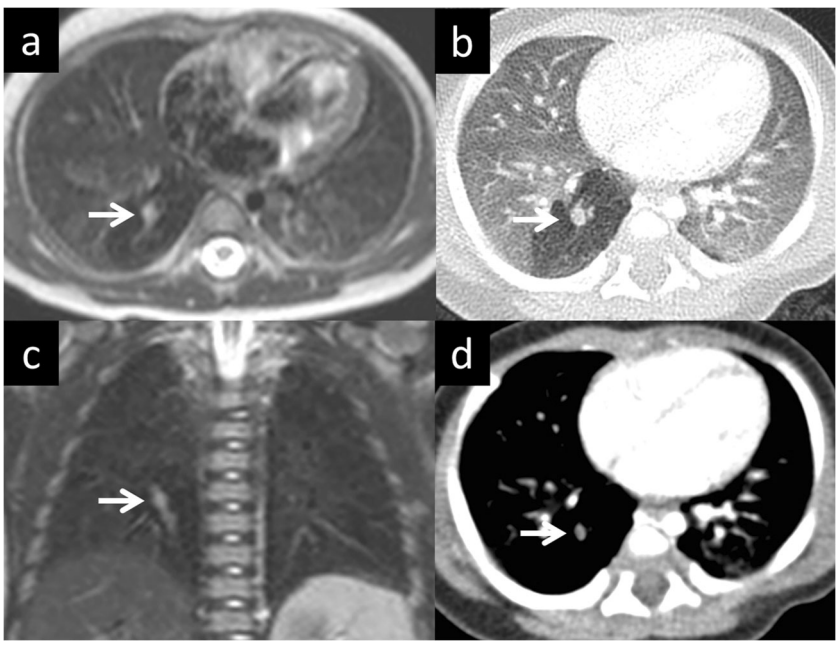

Fig. 2 CT and MR images of bronchial atresia. Axial ss-TSE T2-w (**a**) and axial CT (lung window) (**b**) images show segmental hypointense and hypoattenuated area due to air trapping and decreased vascularity. Coronal MRss-TSE T2-w image (**c**) and axial CT (soft tissue window) (**d**) images better demonstrated the bronchocele (white arrows) within the hypointense and hypoattenuated area, as a tubular-shaped structure in (**c**) and as a solid tissue hypodensity in (**d**)

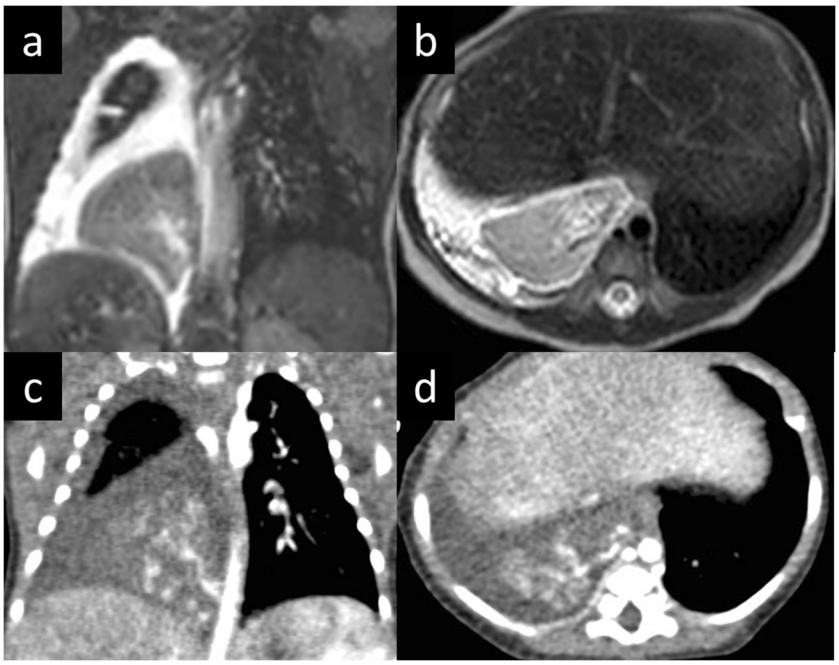

Fig. 3 CT and MR images of extralobar sequestration with a large mass-like lesion located in the right lower hemithorax and an anomalous feeding artery arising from the descending aorta. Coronal MR BFFE (**a**) and axial (**b**) MR ss-TSE T2-w images compared with coronal (**c**) and axial (**d**) CT images; note right pleural effusion

The diagnostic performance of MRI compared with CT for the detection of anomalous arterial vessels was 85.7% sensitivity, 100% specificity, 100% PPV, 94.1% NPV, and 95% accuracy.

The diagnostic performance of MRI compared with CT for the detection of anomalous venous drainage was 57.1% sensitivity, 100% specificity, 100% PPV, 84.2% NPV, and 87% accuracy.

The McNemar-Bowker test showed no statistically significant asymmetry in the marginal proportions between the results of CT and MRI in the evaluation of arterial and venous vessels, with a p value of 0.317 for arterial vessels' detection and 0.083 for venous vessels.

Interobserver agreement

The agreement regarding the relevant elements for diagnosis and the type of CLM was absolute between the two readers ($\kappa = 1.00$, $p < 0.001$).

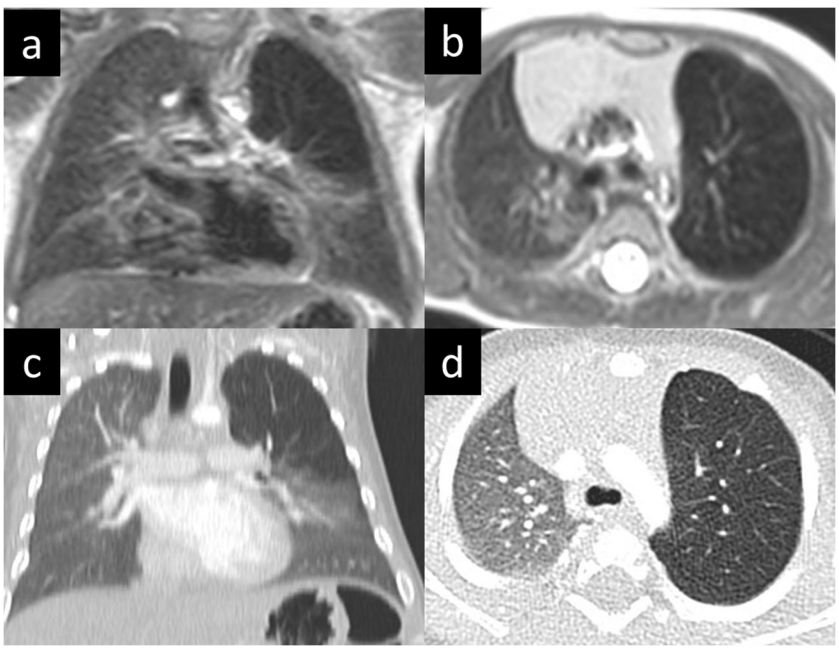

Fig. 4 CT and MR images of congenital lobar overinflation show hyperinflation of the left upper lobe with attenuated lung markings and mediastinal shift to the right side. Coronal (**a**) and axial (**b**) MR ss-TSE T2-w images compared with coronal (**c**) and axial (**d**) CT images

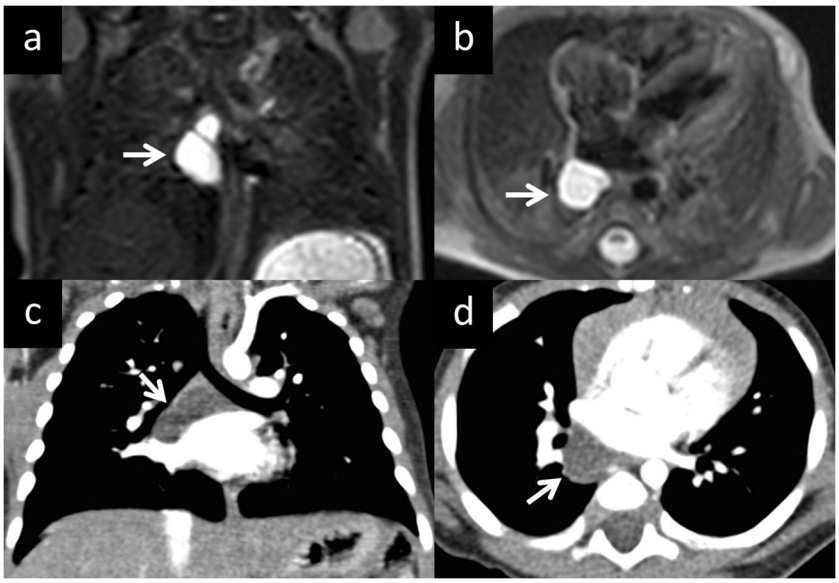

Fig. 5 CT and MR images of bronchogenic cyst. Coronal (**a**) and axial (**b**) MR ss-TSE T2-w images and coronal (**c**) and axial (**d**) CT images show the mediastinal and subcarinal cystic lesion (white arrows)

Discussion

CLMs represent a rare disease with a high clinical variability in postnatal period: they may appear as extended abnormalities, associated with compression of residual lung parenchyma, heart, or vessels, that require immediate surgery or, they can be asymptomatic and incidentally found in adulthood [2, 4].

Most lung malformations are diagnosed in the prenatal period: all patients with a prenatal suspicion of lung malformation must undergo a postnatal contrast-enhanced CT, the gold standard for diagnosis and important for therapeutic planning (surgery or follow-up) [2, 7, 8].

In our hospital, we follow a different protocol for symptomatic or asymptomatic patients. The first undergo contrast-enhanced CT as soon as possible, within the first month of life, to confirm the prenatal diagnosis and to make a preliminary assessment for surgery. Asymptomatic patients usually undergo contrast-enhanced CT within 6 months of life (generally between the third and the sixth month).

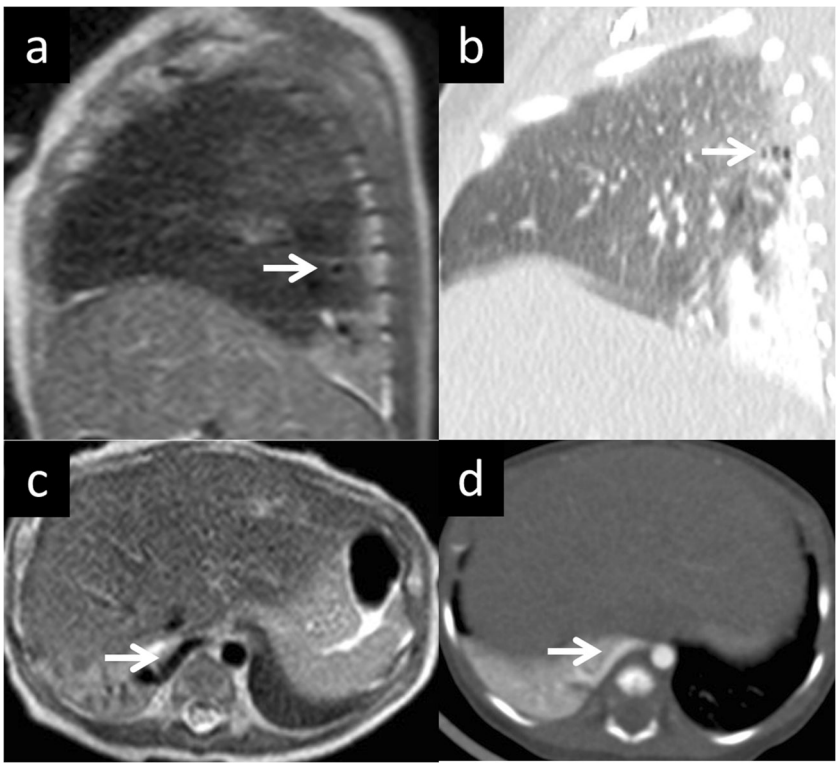

Fig. 6 CT and MR images of hybrid lesion (CPAM + intralobar sequestration). Sagittal MR ss-TSE T2-w (**a**) and CT (**b**) images show areas with different intensity and density due to the presence of solid components and cysts (white arrows) for CPAM and sequestration coexistence. Axial MR ss-TSE T2-w (**c**) and CT maximum intensity projection (**d**) images demonstrated the solid component and the anomalous feeding artery (white arrows) due to the pulmonary sequestration portion of the hybrid malformation

Table 2 Agreement between MRI and CT findings. *TN*, true negative; *TP*, true positive; *FN*, false negative; *FP*, false positive; *PPV*, positive predictive value; *NPV*, negative predictive value

Evaluated elements	TN	TP	FN	FP	Sensitivity	Specificity	Accuracy	PPV	NPV
Presence of cyst	31	9	0	0	100%	100%	100%	100%	100%
Presence of hyperinflation	30	10	0	0	100%	100%	100%	100%	100%
Presence of solid component	33	7	0	0	100%	100%	100%	100%	100%
Presence of abnormal arteries	33	6	1	0	85.7%	100%	95%	100%	94.1%
Presence of abnormal venous drainage	33	4	3	0	57.1%	100%	87%	100%	84.2%
Presence of bronchocele	31	9	0	0	100%	100%	100%	100%	100%

Despite the advantages of CT, such as the short execution time, high spatial resolution, and the highest accuracy in visualizing normal and pathological structures of the lung parenchyma and bronchi, it also carries some disadvantages, mainly the exposure to ionizing radiations. This is a crucial point, especially in the pediatric population, where the number of CT examinations must be reduced whenever possible, performing them only when it is absolutely necessary using a protocol that minimizes exposure to achieve the required diagnostic quality, in accordance with the ALARA (as low as reasonably achievable) principles [21–24]. Contrast-enhanced CT, even if performed with dedicated protocols that provide a dose reduction compared with standard examinations, is not a radiation-free technique. Moreover, in CLM patients, CT is often performed in the neonatal period and mainly within the first year of life: this age group is at an increased risk of stochastic effects determined by ionizing radiation exposure [23–26]. It is estimated that 1 in a 1000 CT examinations will result in a fatal cancer in the pediatric population and that 30% of patients undergo multiple examinations, as in the population we are focusing on [25]. Reducing the number of CT examinations before and after surgery, especially in asymptomatic patients, could significantly reduce the radiation exposure in patients with CLM.

Sedation risk also needs to be weighed against benefits in both CT and MRI. Although good-quality CT images of complex vascular anatomy can be obtained without sedation in neonates with high-end CT scanners [27], unsedated older infants cannot reliably undergo CT acquisitions without the risk of motion artifacts, increased radiation exposure, or missed phases. Risks associated with deep sedation performed by a trained pediatric anesthesiologist are low [28]. Thiopental and dexmedetomidine have been demonstrated to be safe and effective for pediatric imaging [29–31] and are routinely administered in our institution for more than 20 examinations per week. We believe that sedation risk is outweighed or at least balanced by the benefits of an accurate preoperative CT assessment or a reduction in cumulative radiation dose when sedation is performed by a dedicated pediatric anesthesiologist.

Thanks to new scanners and new sequences characterized by very short TE, specific for visualization of lung parenchyma, MRI has recently been considered as a radiation-free alternative to CT in the evaluation of some lung diseases in the pediatric population [15–19, 32, 33].

Currently, there are no published studies regarding the comparison between CT and MRI in the postnatal evaluation of lung malformations: few papers compare CT and MRI in the evaluation of inflammatory disease, cystic fibrosis, or miscellanea [15–19].

In our preliminary prospective study, we wanted to estimate the accuracy of MRI, without contrast medium, compared with the reference standard (contrast-enhanced CT), in the evaluation of CLM, in order to verify if MRI can be an alternative diagnostic tool for this rare disease.

Based on qualitative analysis, MRI allowed a correct diagnosis in 19/20 (95%) patients and the malformation was correctly classified in 22/23 cases (96%). In one patient with diagnosis of sequestration on the CT, MRI was not able to assign a definitive diagnosis suggesting a possible sequestration or CPAM solid lesion or hybrid lesion. On the MRI, a solid lesion was described in the lower left lobe but no anomalous vessels were recognized. On the CT, an anomalous systemic artery arising from the descending aorta and an anomalous vein draining in the hemiazygos vein were detected and, consequently, a diagnosis of sequestration was made. In this case, CT was necessary to obtain a correct definitive diagnosis.

MRI correctly localized all the malformations (Cohen's $k = 1$) and identified all the findings described on the CT except for the abnormal vascularization; thus, MRI resulted comparable with CT in all the cases of malformations that do not exhibit an abnormal vascularization. Considering the seven cases of malformations associated with abnormal vasculature, MRI correctly identified the abnormal vessels in only four cases (57%), while in the remaining 3 cases, MRI was not able to detect the anomalous venous drainage in two of them and neither the abnormal arterial nor venous vascularization in the other. Given the small sample size of our study, there were no statistically significant differences between MRI and CT for vascular evaluation of both arteries and veins. Thus,

considering the vascularization of the lesions, which represents a key feature for surgeons in the preoperative assessment, CT images provided additional relevant diagnostic information to MRI. A direct comparison between contrast-enhanced CT and MRI is needed to fully compare the diagnostic potential of MRI in detecting very small aberrant vessels. CT offered a detailed depiction of the location and course of anomalous vessels which is essential to surgeons in planning resection of CLM and preventing accidental division of anomalous vessels that could result in a fatal outcome from hemorrhage [11]. For this reason, in the setting of CLM located in the lower lobe paravertebral region, the contrast-enhanced CT should be considered routinely in this subset of patients in order to obtain a correct definite diagnosis and allow a complete and precise preoperative planning.

It is important to note that our MRI protocol does not include post contrast images, differently from the CT protocol. We can suppose that MRI lower detection rate of abnormal vessels may be attributable, at least in part, to the absence of contrast medium, which can be used effectively in the identification of abnormal vascularization, especially when dealing with small vessels. Gadolinium-based contrast agents have been demonstrated to be safe in children, but they nonetheless carry a small risk of adverse reactions (0.04%), usually mild [34]. As with current recommendation, gadolinium administration is restricted to congenital heart disease or severe vascular malformation, and some CLMs could be included as well. It is likely that patients with CLM would undergo multiple examinations and therefore the use of contrast needs to be carefully balanced against benefits.

MRI shows values of accuracy, sensitivity, specificity, PPV, and NPV equal to the reference standard in the evaluation of location and presence of cysts, overinflation, bronchocele, and solid components, while in the evaluation of arterial vessels or venous drainage, it shows suboptimal values of sensitivity, accuracy, and NPV compared with the reference standard. MRI could also provide additional information, namely heart function, flow analysis for large vessels, and perfusion evaluation [35–37], making it a valuable tool for morpho-functional preoperative assessment in selected cases. Flow analysis could be performed selectively on the right and left pulmonary arteries with phase-contrast sequences providing valuable information in the preoperative setting. In selected cases with combined pulmonary and cardiac malformations, cine MRI can provide a comprehensive evaluation of pulmonary regurgitation or stenosis and left and right ventricular function. In our institution ultra-short echo time (UTE) imaging was unfortunately not available. UTE imaging, along with other recent advances in lung imaging, will make the choice of MRI in younger patients even more compelling [36].

Our study, however, has some limitations. First, it is a single-center study and the number of subjects studied is relatively low. As previously mentioned, the comparison between MRI and CT in arterial and venous vascular analysis failed to demonstrate significant differences, at least in part, due to the small sample size. Large prospective studies should be performed to confirm the accuracy of MRI in the diagnosis of CLM, exploring the full potential of the most recent technological advances. Secondly, we have not assessed the potential benefits of the MRI in the follow-up of CLM. Moreover, we performed unenhanced MRI comparing it with contrast-enhanced CT, limiting the diagnostic potential of MRI in the diagnosis of malformations, especially vascular lesions. Another possible limitation was the time gap between MRI and CT acquisitions in our series; however, we did not find significant differences when comparing MRI and CT performed close to each other and those performed farther apart.

Conclusion

In conclusion, our study, although preliminary, shows that unenhanced MRI could represent a valid alternative in the postnatal diagnosis and management of CLM, allowing an accurate diagnosis of location and characterization of these malformations avoiding radiation exposure and intravenous contrast administration. Nevertheless, in the subset of patients with lesions located in the lower lobe paravertebral region, contrast-enhanced CT still represents the exam of choice to study the vascularization of the malformation being of potential benefit to referring surgeons for preoperative planning.

Funding The authors state that this work has not received any funding.

Compliance with ethical standards

Guarantor The scientific guarantor of this publication is Dr. Salvatore Zirpoli.

Conflict of interest The authors of this manuscript declare no relationships with any companies, whose products or services may be related to the subject matter of the article.

Statistics and biometry No complex statistical methods were necessary for this paper.

Informed consent Written informed consent was obtained from all subjects (patients) in this study.

Ethical approval Institutional Review Board approval was obtained.

Methodology
- prospective
- diagnostic or prognostic study
- performed at one institution

References

1. Wall J, Coates A (2014) Prenatal imaging and postnatal presentation, diagnosis and management of congenital lung malformations. Curr Opin Pediatr 26:315–319. https://doi.org/10.1097/MOP.0000000000000091
2. Thacker PG, Rao AG, Hill JG, Lee EY (2014) Congenital lung anomalies in children and adults. Current concepts and imaging findings. Radiol Clin North Am 52:155–181. https://doi.org/10.1016/j.rcl.2013.09.001
3. Irodi A, Prabhu SM, John RA, Leena R (2015) Congenital bronchopulmonary vascular malformations, "sequestration" and beyond. Indian J Radiol Imaging 25:35–43. https://doi.org/10.4103/0971-3026.150138
4. Costa Júnior Ada S, Perfeito JA, Forte V (2008) Surgical treatment of 60 patients with pulmonary malformations: what have we learned? J Bras Pneumol 34:661–666. https://doi.org/10.1590/S1806-37132008000900005
5. Lee EY, Dorkin H, Vargas SO (2011) Congenital pulmonary malformations in pediatric patients: review and update on etiology, classification, and imaging findings. Radiol Clin North Am 49:921–948. https://doi.org/10.1016/j.rcl.2011.06.009
6. Peters RT, Burge DM, Marven SS (2013) Congenital lung malformations: An ongoing controversy. Ann R Coll Surg Engl 95(2):144–7. https://doi.org/10.1308/003588412X13373405387735
7. Azizkhan RG, Crombleholme TM (2008) Congenital cystic lung disease: contemporary antenatal and postnatal management. Pediatr Surg Int 24:643–657. https://doi.org/10.1007/s00383-008-2139-3
8. Epelman M, Kreiger PA, Servaes S, Victoria T, Hellinger JC (2010) Current imaging of prenatally diagnosed congenital lung lesions. Semin Ultrasound CT MRI 31:141–157. https://doi.org/10.1053/j.sult.2010.01.002
9. Lee EY, Boiselle PM, Cleveland RH (2008) Multidetector CT evaluation of congenital lung anomalies. Radiology 247:632–648. https://doi.org/10.1148/radiol.2473062124
10. Tomà P, Rizzo F, Stagnaro N, Magnano G, Granata C (2011) Multislice CT in congenital bronchopulmonary malformations in children. Radiol Med 116:133–151. https://doi.org/10.1007/s11547-010-0582-4
11. Lee EY, Tracy DA, Mahmood SA, Weldon CB, Zurakowski D, Boiselle PM (2011) Preoperative MDCT evaluation of congenital lung anomalies in children: comparison of axial, multiplanar, and 3D images. AJR Am J Roentgenol 196:1040–1046. https://doi.org/10.2214/AJR.10.5357
12. Pauwels EK, Bourguignon M (2011) Cancer induction caused by radiation due to computed tomography: a critical note. Acta Radiol 52:767–773. https://doi.org/10.1258/ar.2011.100496
13. Pearce MS, Salotti JA, Little MP et al (2012) Radiation exposure from CT scans in childhood and subsequent risk of leukaemia and brain tumours: a retrospective cohort study. Lancet 380:499–505. https://doi.org/10.1016/S0140-6736(12)60815-0
14. Sodhi KS, Lee EY (2014) What all physicians should know about the potential radiation risk that computed tomography poses for paediatric patients. Acta Paediatr 103:807–811. https://doi.org/10.1111/apa.12644
15. Gorkem SB, Coskun A, Yikilmaz A, Zurakowski D, Mulkern RV, Lee EY (2013) Evaluation of pediatric thoracic disorders: comparison of unenhanced fast-imaging-sequence 1.5-T MRI and contrast-enhanced MDCT. AJR Am J Roentgenol 200:1352–1357. https://doi.org/10.2214/AJR.12.9502
16. Wielpütz MO, Heußel CP, Herth FJ, Kauczor HU (2014) Radiological diagnosis in lung disease: factoring treatment options into the choice of diagnostic modality. Dtsch Arztebl Int 111:181–187. https://doi.org/10.3238/arztebl.2014.0181
17. Sodhi KS, Khandelwal N, Saxena AK et al (2016) Rapid lung MRI in children with pulmonary infections: time to change our diagnostic algorithms. J Magn Reson Imaging 43:1196–1206. https://doi.org/10.1002/jmri.25082
18. Tepper LA, Ciet P, Caudri D, Quittner AL, Utens EM, Tiddens HA (2016) Validating chest MRI to detect and monitor cystic fibrosis lung disease in a pediatric cohort. Pediatr Pulmonol 51:34–41. https://doi.org/10.1002/ppul.23328
19. Dournes G, Menut F, Macey J et al (2016) Lung morphology assessment of cystic fibrosis using MRI with ultra-short echo time at submillimeter spatial resolution. Eur Radiol 26:3811–3820. https://doi.org/10.1007/s00330-016-4218-5
20. Stocker JT (2002) Congenital pulmonary airway malformation: a new name for and an expanded classification of congenital cystic adenomatoid malformation of the lung. Histopathology 41(suppl2):424–430
21. Paterson A, Frush DP (2007) Dose reduction in paediatric MDCT: general principles. Clin Radiol 62:507–517. https://doi.org/10.1016/j.crad.2006.12.004
22. Greenwood TJ, Lopez-Costa RI, Rhoades PD et al (2015) CT dose optimization in pediatric radiology: a multiyear effort to preserve the benefits of imaging while reducing the risks. Radiographics 35:1539–1554. https://doi.org/10.1148/rg.2015140267
23. Callahan MJ (2011) CT dose reduction in practice. Pediatr Radiol 41(Suppl 2):488–492. https://doi.org/10.1007/s00247-011-2099-y
24. Brenner DJ, Elliston CD, Hall EJ, Berdon WE (2001) Estimated risks of radiation-induced fatal cancer from pediatric CT. AJR Am J Roentgenol 176:289–296. https://doi.org/10.2214/ajr.176.2.1760289
25. Frush DP, Donnelly LF, Rosen NS (2003) Computed tomography and radiation risks: what pediatric health care providers should know. Pediatrics 112:951–957. https://doi.org/10.1542/peds.112.4.951
26. Slovis TL (2003) Children, computed tomography radiation dose, and the As Low As Reasonably Achievable (ALARA) concept. Pediatrics 112:971–972. https://doi.org/10.1542/peds.112.4.971
27. Han BK, Overman DM, Grant K et al (2013) Non-sedated, free breathing cardiac CT for evaluation of complex congenital heart disease in neonates. J Cardiovasc Comput Tomogr 7:354–360. https://doi.org/10.1016/j.jcct.2013.11.006
28. Krauss B, Green SM (2006) Procedural sedation and analgesia in children. Lancet 367:766–780. https://doi.org/10.1016/S0140-6736(06)68230-5
29. Beekman RP, Hoorntje TM, Beek FJ, Kuijten RH (1996) Sedation for children undergoing magnetic resonance imaging: efficacy and safety of rectal thiopental. Eur J Pediatr 155:820–822. https://doi.org/10.1007/BF02002915
30. Alp H, Güler I, Orbak Z, Karakelleoğlu C, Tan H, Eren S (1999) Efficacy and safety of rectal thiopental: sedation for children undergoing computed tomography and magnetic resonance imaging. Pediatr Int 41:538–541. https://doi.org/10.1046/j.1442-200x.1999.01124.x
31. Mason KP, Zurakowski D, Zgleszewski SE et al (2008) High dose dexmedetomidine as the sole sedative for pediatric MRI. Paediatr Anaesth 18:403–411. https://doi.org/10.1111/j.1460-9592.2008.02468.x
32. Biederer J, Mirsadraee S, Beer M et al (2012) MRI of the lung (3/3)-current applications and future perspectives. Insights Imaging 3:373–386. https://doi.org/10.1007/s13244-011-0142-z
33. Wild JM, Marshall H, Bock M et al (2012) MRI of the lung (1/3): methods. Insights Imaging 3:345–353. https://doi.org/10.1007/s13244-012-0176-x
34. Sundgren PC, Leander P (2011) Is administration of gadolinium-based contrast media to pregnant women and small children justified? J Magn Reson Imaging 34(4):750–7. https://doi.org/10.1002/jmri.22413

35. Groves AM, Chiesa G, Durighel G et al (2011) Functional cardiac MRI in preterm and term newborns. Arch Dis Child Fetal Neonatal Ed 96:86–91. https://doi.org/10.1136/adc.2010.189142
36. Tiddens HAWM, Kuo W, van Straten M, Ciet P (2018) Paediatric lung imaging: the times they are a-changin'. Eur Respir Rev 27:1–9. https://doi.org/10.1183/16000617.0097-2017
37. Weis M, Zoellner FG, Hagelstein C et al (2016) Lung perfusion MRI after congenital diaphragmatic hernia repair in 2-year-old children with and without extracorporeal membrane oxygenation therapy. AJR Am J Roentgenol 206:1315–1320. https://doi.org/10.2214/AJR.15.14860